Tribology International 216 (2026) 111592

Contents lists available at ScienceDirect

Tribology International

journal homepage: www.elsevier.com/locate/triboint

Friction behavior of grease-lubricated rolling contact and its dependence on grease film under starvation

Shuo Zhang [a,*], Benjamin Klinghart [a], Georg Jacobs [a], Jianlong Xiao [a], Yujun Wang [a], Florian König [a,b], Marius Bürger [a]

[a] Institute for Machine Elements and Systems Engineering, RWTH Aachen University, Schinkelstrasse 10, Aachen 52062, Germany
[b] Soete Laboratory, Ghent University, 9052 Ghent, Belgium

ARTICLE INFO

Keywords:
Grease
Rolling contact
Friction
Film thickness
Starvation

ABSTRACT

Owing to the widespread use of grease-lubricated rolling bearings, friction losses remain a significant concern. When evaluating friction behavior, ball-on-disk tribometer tests are typically conducted under fully flooded conditions, whereas the grease supplied to the contacts in a rolling bearing is often starved. This study aims to determine whether grease supply conditions affect friction behavior and to clarify the correlation between friction behavior and the grease film under starved conditions. To achieve this aim, two tribometers are used to measure friction behavior and film thickness, respectively. The results show that the friction behavior under fully flooded conditions is not representative of that under starved conditions, due to variations in film formation. Under starved conditions, the traction coefficient is more sensitive to operating conditions and depends on the thickness and both components of the grease film.

1. Introduction

Approximately 20 % of the world's total energy is consumed to overcome friction in tribological contacts, including those in various rolling bearings [1]. In rolling bearings, the friction losses are strongly influenced by the characteristics of the lubricating film [2]. Among various lubricants, grease is used in more than 90 % of rolling bearing lubrication applications [3]. Therefore, elucidating the friction behavior of grease-lubricated rolling bearings under various operating conditions provides insights into improving the frictional performance of bearing greases.

Although grease-lubricated rolling bearings are widely used, there is only a limited number of published studies on the friction behavior, as summarized in [4,5]. Among these limited studies, the ball-on-disk tribometer has emerged as one of the most widely employed experimental setups [5–12]. This popularity is primarily due to its ability to control key operating parameters and thereby enable deeper insights into mechanisms [11,13]. These advantages make it particularly suitable for simulating the contact conditions typically encountered in practical rolling bearing applications. Therefore, ball-on-disk tribometer test is considered as a modern method for evaluating the friction behavior and lubrication mechanisms of grease-lubricated rolling bearings [4].

Tribometer testing methods have not yet been formally standardized [4]. When evaluating the friction behavior, tribometer tests typically utilize a scoop to maintain continuous re-lubrication of the contact [5–11]. Therefore, the contact inlet is always fully supplied with grease, which is referred to as a fully flooded condition [12,14]. Grease primarily consists of a thickener network and base oil, which behave as a plastic solid and a Newtonian fluid, respectively [15]. Under fully flooded conditions, grease is squeezed and sheared in the contact area and becomes a homogeneous glomerate of thickener and oil [16], as shown in Fig. 1(a). During high-speed operations, high shear rates lead to severe shear thinning of the thickener network such that the grease viscosity within the contact area approaches that of base oil viscosity [15,17]. Consequently, the grease film thickness is comparable to that of base oil and increases with increasing rolling speed [14,18]. In contrast, under low-speed conditions, the shear stress is relatively low. Therefore, the thickener network maintains a viscosity much higher than that of the base oil, thereby flowing more slowly than the base oil within the contact zone [15,19]. This leads to an increase in thickener concentration in the contact area [15,17,20], and consequently, an increase in grease viscosity [15,21]. Consequently, during low-speed operations, the grease film thickness is much higher than that of base oil and increases

* Corresponding author.
E-mail address: shuo.zhang@imse.rwth-aachen.de (S. Zhang).

https://doi.org/10.1016/j.triboint.2025.111592
Received 10 July 2025; Received in revised form 10 December 2025; Accepted 17 December 2025
Available online 18 December 2025

with decreasing rolling speed. In summary, under fully flooded conditions, the grease film thickness typically exhibits a V-shaped curve as rolling speed increases [7,22]. Correspondingly, the friction behavior above the transition speed is governed by base oil type and its viscosity [5,10]. For a given oil type, the friction coefficient reduces with increasing temperature [5]. In contrast, below the transition speed, friction behavior is highly dependent on thickener type [8,11]. It may exhibit lower friction coefficients compared to those observed for base oils because thicker grease films reduce risks of asperity contacts [8,9,11].

In contrast to the tribometer test, grease lubrication in practical rolling bearings usually has two phases: the churning phase and the bleeding phase [23–25]. During the churning phase, some fresh grease is entrained into the contact area, while most of the grease is displaced to the track side [26]. The entrained grease can gradually form a solid-like thickener-rich layer as overrolling continues [16,27–31]. The churning phase usually is indicated by a rapid decrease in film thickness [14,25,31]. After the churning phase, the displaced grease cannot reflow back into the raceway without an external force due to its yield stress. Although certain aspects of bearing design and operation (spin, vibration, cage effects) that could promote the intermittent reflow of bulk grease into the track [32], the grease supplied to contact inlet in practical rolling bearings is often insufficient and starved [3,33]. Under starved conditions, the displaced grease usually acts as reservoir, which can slowly release oil to the track due to centrifugal force [34], gravity [35] or capillary force [36,37]. This process is referred to as oil bleeding. This bled oil can contribute to the separation of contacting surfaces by forming an elastohydrodynamic lubrication (EHL) film [31]. The thickness of oil film is closely related to the bleeding property of grease and operating conditions [14,16,25,31,32]. Depending on the formation of oil film, the total grease film thickness during bleeding phase can be slightly decreased, remain constant, or recover [23–25,31,38]. Consequently, the grease film under starved condition is composed of both the thickener-rich layer and the oil film induced by bled oil, as schematically shown in Fig. 1(b).

In summary, when evaluating the friction behavior of grease lubrication, ball-on-disk tribometer tests are typically conducted under fully flooded conditions. In contrast, grease-lubricated rolling bearings generally operate under starved conditions. The formation of the grease film under starved conditions differs from that under fully flooded conditions. Under starved conditions, the grease film consists of two components (thickener-rich layer and oil film, as shown in Fig. 1), whereas under fully flooded conditions, it is homogeneous. Therefore, variations in grease supply conditions may introduce uncertainties when extrapolating friction behavior from tribometer tests to real bearing applications. However, a comprehensive study on the effect of supply conditions on friction behavior using tribometers is still lacking. Moreover, understanding the dependence of friction behavior on the grease film is essential for identifying potential strategies to improve the friction performance of bearing greases [5]. Under fully flooded conditions, the dependence of friction behavior on grease film has been clarified in [5,8–11]. However, under starved conditions, this dependence remains unclear due to the lack of understanding of friction behavior [9].

To address both of the aforementioned questions, this study aims to elucidate the influence of grease supply conditions on friction behavior and to clarify the correlation between friction and grease film under starved condition. To achieve this aim, first, friction behavior under fully flooded and starved conditions is evaluated for various greases and under different operating conditions. Subsequently, the grease film thickness under starved condition is measured and correlated with the friction behavior.

2. Martials and methods

2.1. Tested lubricants

Three greases are tested in this study, and their properties are listed in Table 1. These greases are composed of the same base oil but differ in thickener type. The selection of greases is primarily based on their popularity in rolling bearing applications. Lithium-thickened greases are the most widely used, whereas polyurea-thickened greases are regarded as potential alternatives. Therefore, one grease with a simple lithium thickener, one with a complex lithium thickener, and one with a polyurea thickener are studied. The thickener concentrations are selected from commercially used thickener-base oil combinations to achieve a consistency of NLGI classes 2–3, which are commonly used in rolling bearing applications [33]. As a benchmark, the properties of the base oil are also listed. The primary focus of this study is to clarify the friction behavior under different grease supply conditions; therefore, no additives are included in all greases and base oil. To isolate the influence of the thickener and the base oil, the friction behavior of base oil is measured separately.

Table 1
Parameters for tested lubricants.

Lubricants	Li-S-PAO	Li-C-PAO	PU-PAO	PAO
NLGI	2	3	2	-
Base oil	PAO	PAO	PAO	-
Base oil viscosity	98.0 cSt (40°C); 22.1 cSt (80°C)			
Viscosity-pressure coefficient	15 GPa^{-1} (40°C)			
Thickener	Lithium-simple	Lithium-complex	Polyurea	-
Thickener concentration	9.5 %	14.5 %	14.1 %	0

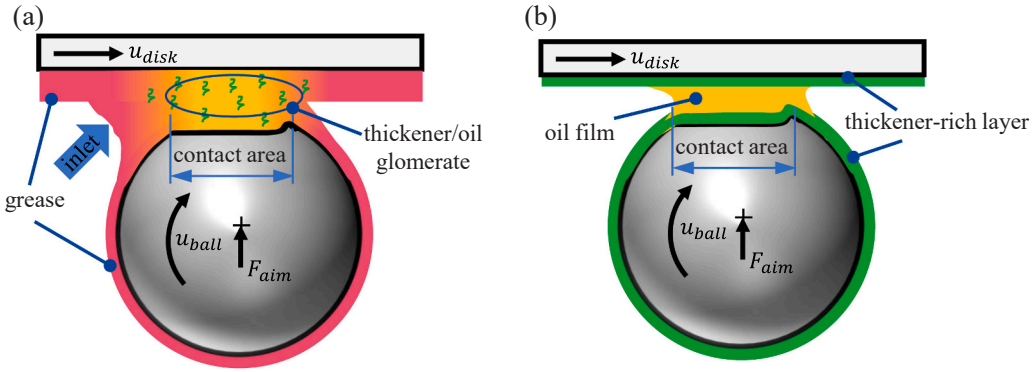

Fig. 1. Schematic of lubricating film components under two supply conditions, (a) fully flooded condition, (b) starved condition.

2.2. Friction measurement

In this study, the Mini Traction Machine (MTM), a ball-on-disk tribometer from PCS Instruments is used to measure traction coefficient in grease-lubricated rolling contacts. Within the MTM tribometer, a ball is loaded against a flat disk to form a point contact. The ball and disk can rotate independently, allowing various slide-roll ratios. The traction force at the contact is measured using a torque transducer mounted between the ball housing and a fixed reference point. The load, rotational speed, and temperature are controllable, enabling a traction measurement under different conditions. More details of MTM tribometer have been introduced in [5–12,39].

The measurement process used in this study is shown in Fig. 2. As shown in Fig. 2(a), a grease applicator from PCS Instruments is used to ensure a consistent amount of grease for all conditions and to minimize the waste of grease. This applicator has 12 evenly distributed holes, through which grease droplets can be deposited onto the center of the disk track, as illustrated in Fig. 2(b).

After applying the grease, the MTM and the specimens, including the ball and the disk with the applied grease, are preheated to the targeted operating temperature. The MTM is heated using electrical cartridge heaters located in the channels of the lubrication pot, as detailed in [39]. The heating time varies depending on the targeted temperature. If the specimens are heated inside of MTM, the evaporation of base oil from the grease sample cannot be effectively controlled, practically at higher temperatures [40]. To eliminate this uncertainty, the testing specimens are preheated separately in an oven for 10 min to reach the operating temperature under all operating conditions in this study.

After preheating, the specimens are assembled onto the MTM. To ensure a consistent grease distribution, the grease is uniformly redistributed before tests using a grease scoop. The grease scoop is a PTFE assembly from PCS Instruments, which can collect and redistribute grease onto the track center [5]. The redistributed grease on the disk is shown in Fig. 2(c).

After redistribution, the traction coefficients are measured under two grease supply conditions. Under fully flooded condition, the test procedure in this study is similar to that described in [5,6,10]. The grease scoop remains assembled on the MTM during testing. This setup allows grease to be fed through the contact sufficiently and continuously, as shown in Fig. 2(d). In contrast, under starved condition, grease scoop is removed from the MTM after redistribution, so that the grease can be displaced to the track side by overrolling, as shown in Fig. 2(e).

The measurement of traction coefficient under fully flooded condition is repeated at least once to verify the repeatability. In contrast, the measurement under starved condition is repeated at least twice because of the poor repeatability [5]. For each operating condition new specimens (including disk and ball) are used.

2.3. Grease film thickness measurement

In this study, the ball-on-disk tribometer EHD2 from PCS Instruments is used to measure grease film thickness. The basic working principle of EHD2 is similar to that of the MTM, except that a glass disk is used. Additionally, a spectrometer is used to record the interference pattern generated by two light beams reflected from the bottom of the glass disk and the surface of the steel ball, respectively. Based on the recorded interference pattern, the central film thickness can be calculated [41]. Further details about the EHD2 tribometer are available in [14,42].

The measurement process using the EHD2 tribometer is shown in Fig. 3. Similar to traction measurement, fresh grease is applied to the glass disk using a grease applicator prior to the measurement, as shown in Fig. 3(a). Additionally, the applicator is used to distribute the grease uniformly on the disk. Afterwards, a narrow section of the disk, approximately 1.0 cm wide, is cleaned manually to remove the grease from that area. This action is designed to establish a reference point for measuring film thickness on the EHD2 tribometer [41].

After distributing, the specimens are preheated in an oven to the targeted operating temperature, following a procedure similar to that used for traction measurements. Simultaneously, the EHD2 tribometer is heated using its internal heaters. Subsequently, the heated disk is assembled into the tribometer, as shown in Fig. 3(b).

Once assembled, the tests are conducted under starved condition across various operating parameters. During overrolling, the grease is pushed by the ball to the track sides. Meanwhile, the grease film thickness, which is a superposition of the thickener-rich layer and the oil film, is measured using the spectrometer. Each grease film thickness test is conducted three times, utilizing a new ball specimen and a new track position on the disk for each trial.

Besides measuring the grease film thickness, the thickness of thickener-rich layers can also be assessed. The oil film is an EHL film that only forms between moving surfaces [43]. At the end of each test, the motor is halted, causing the oil film thickness to decrease to zero [16,42]. In contrast, the thickness of the thickener-rich layer remains unchanged by rolling speed once formed [43]. Consequently, the thickness of the thickener-rich layer can be evaluated at a standstill and under operating load conditions, after each measurement of grease film thickness.

The thickener-rich layer can be formed on both contacting surfaces [38,42]. The measurement methods for the thickness of the thickener-rich layer on each surface are shown separately in Fig. 3(c) and (d). As shown in Fig. 3(c), the thickness of the thickener-rich layer on the ball is first measured on the cleaned area of the disk, with the

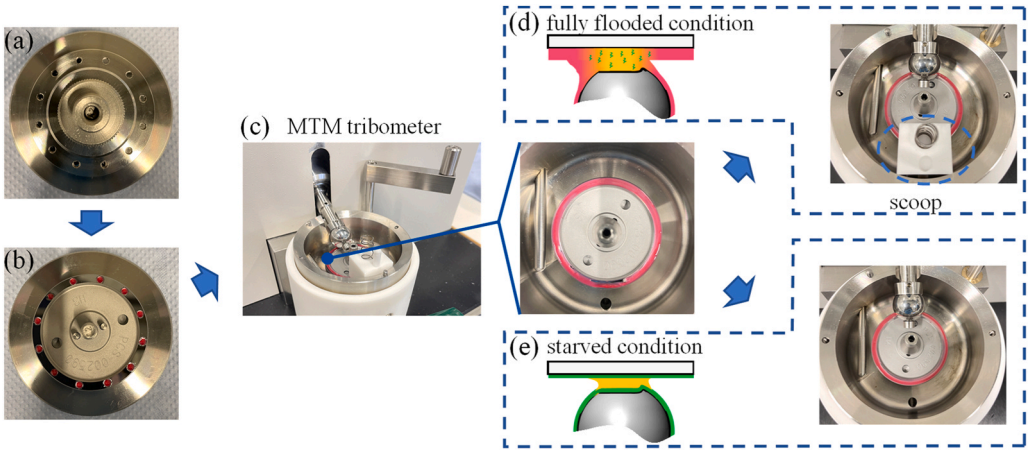

Fig. 2. Measurement process of traction coefficient using MTM, (a) grease applicator for MTM; (b) grease droplets on disk; (c) MTM tribometer; (d) setup for measuring traction coefficient under fully flooded condition; (e) setup for measuring traction coefficient under starved condition.

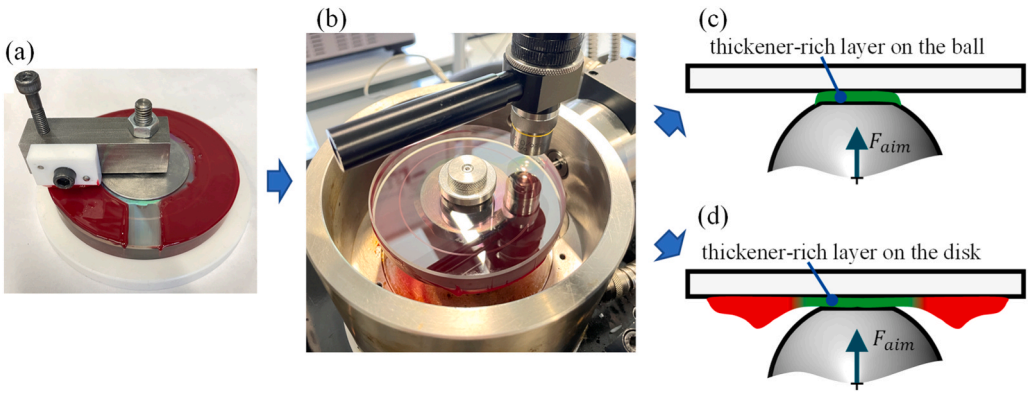

Fig. 3. Measurement process of grease film thickness using EHD2, (a) grease applicator for EHD2; (b) EHD2 tribometer; (c) setup for measuring the thickness of thickener-rich layer on the ball; (d) setup for measuring the thickness of thickener-rich layer on the disk.

tribometer at standstill and under operating load. Subsequently, the thickness of the thickener-rich layer on the disk is measured using a cleaned ball, as shown in Fig. 3(d). This measurement is performed at six points along the corresponding track, with the tribometer at standstill and under the operating load. Prior to each measurement, the ball is cleaned. Additional information regarding the measurement of the thickener-rich layer can be found in [44]. To the best of the authors' knowledge, this testing method for the thickener-rich layer was first proposed by Cann [16], and subsequently employed by other researchers [18,22,42].

2.4. Operating conditions

The operating and contact parameters used in this study are listed in Table 2. The disk materials used in MTM and EHD2 tribometers are different. The maximum contact pressure attainable with the EHD2 is 0.7 GPa. Applying the same contact pressure to MTM results in an insufficient load (approximately 12.5 N). Under this load, the measured traction coefficient exhibits drift during overrolling, leading to significant errors, particularly during extended test durations [39]. Therefore, the contact pressure on MTM is set to 0.9 GPa. A similar approach is also adopted in [10]. When the scoop is removed, no mechanism promotes the reflow of displaced grease after churning. Therefore, the lubrication condition is generally considered to be starved [16,27]. However, if the test duration is too short or the rolling speed is too low, the residual grease on the track may still be sufficient to achieve a fully flooded condition. Therefore, these two parameters must be chosen carefully. In this study, 5000 disk revolutions are chosen based on our previous experience in [14,42] and also on the results in [12,25,31]. The rolling speeds are selected primarily on the basis of results reported by Fischer [45]. He used similar greases to those in this study and showed that grease film thickness started to decrease above 200 mm/s. Therefore, two relatively high rolling speeds, 200 mm/s and 600 mm/s, are selected. As temperature is the most influential factor in grease lubrication [46], two operating temperatures are selected. A direct in-situ measurement of the grease temperature is not feasible during testing. Instead, the air temperature adjacent to the disk and grease can be measured by the Lube Temp Probe. Although the grease temperature during operating may be slightly lower than this measured temperature, the difference between the grease temperature and the measured temperature is expected to be negligible due to preheating and the PTFE cover. Therefore, the temperature measured by the Lube Temp Probe is used as the indicator of the operating temperature in this study. To study the correlation between traction behavior and film thickness, the test duration for traction measurement is set to 5000 disk revolutions, matching that used in the film thickness tests [24].

Table 2
Operating and contact parameters.

Parameter [Unit]	MTM tribometer	EHD2 tribometer
Radius of ball specimen, R_{ball}	9.525 mm	
Elastic modulus of ball, E_{ball}	207 GPa	
Poisson's ratio of ball, ν_{ball}	0.29	
Elastic modulus of disk, E_{disk}	207 GPa	75 GPa
Poisson's ratio of disk, ν_{disk}	0.29	0.22
Maximum Hertzian pressure, p_{Hz}	0.9 GPa	0.7 GPa
Radius of disk track, R_{track}	21.2 mm	38.5 mm
Critical film thickness between fully film lubrication and mixed lubrication, $h_\lambda = 3\sqrt{\sigma_{disk}^2 + \sigma_{ball}^2}$	28.7 nm	18.5 nm
Operating temperature, T	40°C and 80°C (Lube Temp Probe)	
Rolling speed, $u_r = \frac{u_{disk} + u_{ball}}{2}$	200 mm/s and 600 mm/s	
Slide/roll ratio, $SRR = \frac{u_{disk} - u_{ball}}{u_r}$	0	
Test duration	5000 disk revolutions	
	approx. 56 min at 200 mm/s; approx. 19 min at 600 mm/s	approx. 90 min at 200 mm/s; approx. 30 min at 600 mm/s

3. Results and discussion

In the following two sections, first, the effect of supply conditions on friction behavior during overrolling and on stable friction behavior are presented. Subsequently, the dependence of friction behavior on grease film under starved conditions is discussed.

3.1. Effect of supply conditions on friction behavior

3.1.1. On friction behavior during overrolling

The friction behavior during overrolling under two supply conditions is compared using Li-C-PAO as a representative example to avoid extensive repetition, because all three greases tested in this study show similar behaviors. The traction coefficients for two other greases are provided in the Appendix 5.1. The traction coefficients at a given operating temperature and rolling speed are shown in Fig. 4. At the beginning of overrolling, the traction coefficients under both fully flooded and starved conditions are comparable. During the initial stage of overrolling (approximately 500 disk revolutions), the traction coefficient under fully flooded condition shows an oscillation and then becomes stable until the end of the measurement. Throughout the test duration, the traction coefficient varies only slightly under fully flooded conditions. The variation range is approximately 0.014. A similar traction behavior, including the oscillation, is also reported by Cann under fully flooded conditions [12].

In contrast, the traction coefficient under starved condition varies

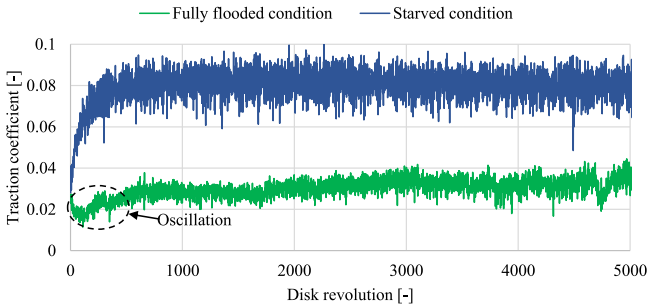

Fig. 4. Traction coefficients during overrolling under two supply conditions (Li-C-PAO; u_r=200 mm/s; T = 40°C).

significantly during overrolling. The variation range is approximately 0.052. It increases rapidly, then becomes stable after approximately 700 disk revolutions. The stable traction coefficient is significantly higher than that observed under fully flooded condition.

The traction coefficients at a higher temperature are shown in Fig. 5. Similar traction behavior under both supply conditions is also observed at the beginning of overrolling. Under fully flooded condition, the traction coefficient remains nearly constant throughout overrolling, except for an initial oscillation at the beginning of the test. The variation range is approximately 0.018.

In contrast, the traction coefficient under starved condition increases significantly during the first approximately 300 disk revolutions. The variation range is approximately 0.035. Compared to that at a lower temperature (40°C, as shown in Fig. 4), the traction coefficient at a higher temperature gradually decreases until the end of the measurement. Additionally, under starved condition, although the traction behavior varies with temperature, the maximum traction coefficient during overrolling remains consistent across both tested temperatures.

The effects of supply conditions on the traction coefficient at a higher rolling speed (u_r=600 mm/s) and under two operating temperatures are shown in Fig. 6 and Fig. 7, respectively. Similar to the results at 200 mm/s, the grease supply condition does not significantly affect the traction coefficient at the beginning of overrolling. Shortly after, the traction coefficients begin to diverge under two supply conditions as overrolling continues. Specifically, under fully flooded condition, the traction coefficient varies slightly, whereas under starved condition, it exhibits significant variation. Under starved condition, the traction coefficient at 40°C remains nearly constant after approximately 2000 disk revolutions, while that at 80°C begins to decrease after approximately 1000 revolutions. Notably, under starved conditions, the maximum traction coefficient during overrolling is not significantly affected by rolling speed or operating temperature, and remains approximately 0.08.

3.1.2. *On friction behavior under stable state*

To quantitatively evaluate the effect of supply conditions on friction

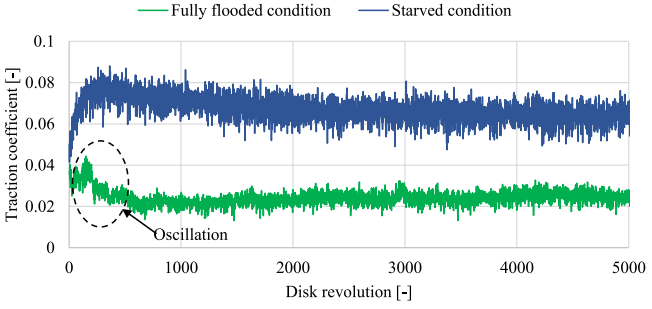

Fig. 5. Traction coefficients during overrolling under two supply conditions (Li-C-PAO; u_r=200 mm/s; T = 80°C).

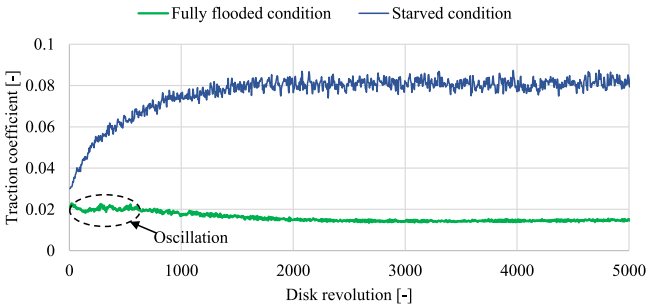

Fig. 6. Traction coefficients during overrolling under two supply conditions (Li-C-PAO; u_r=600 mm/s; T = 40°C).

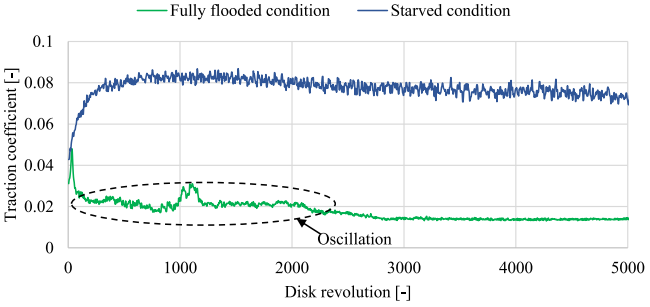

Fig. 7. Traction coefficients during overrolling under two supply conditions (Li-C-PAO; u_r=600 mm/s; T = 80°C).

behavior, the stable traction coefficients under various conditions and greases are compared in this subsection. The stable traction coefficient in this study is defined as the average value between 4500 and 5000 disk revolutions. To better understand the lubrication condition, the traction coefficient of the base oil is also measured.

The stable traction coefficients under fully flooded condition are shown in Fig. 8. Under this condition, the traction coefficients of greases are comparable to that of the base oil. Specifically, at a lower rolling speed (200 mm/s, see Fig. 8a), the traction coefficients of grease lubrication are slightly higher than those of the base oil, expect for Li-C-PAO

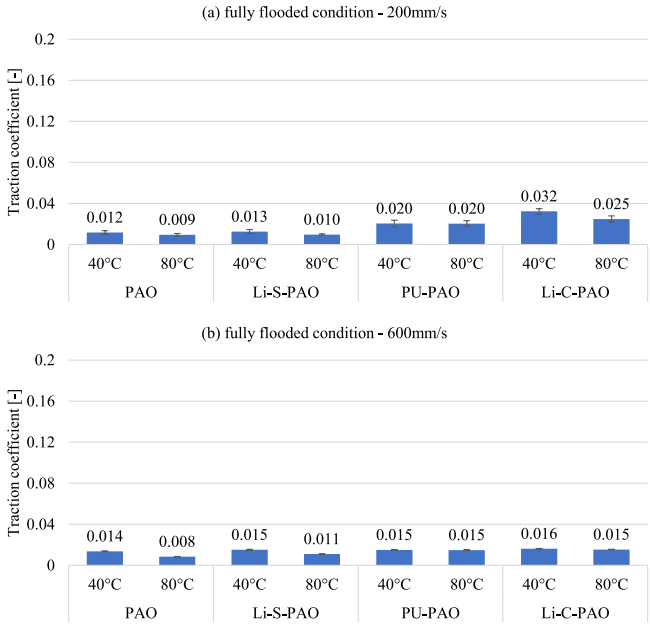

Fig. 8. Stable traction coefficient under fully flooded conditions, (a) u_r= 200 mm/s, (b) u_r= 600 mm/s.

due to its high thickener concentration. When the rolling speed increases to 600 mm/s (see Fig. 8b), the traction coefficients of grease and oil lubrication are nearly identical. Additionally, the traction coefficients of all tested greases and the base oil decrease as the operating temperature increases from 40°C to 80°C. These observations are consistent with results from Laurentis et al. [5,10], who also reported that the traction coefficient under fully flooded grease lubrication is comparable to that under oil lubrication and decreases at elevated temperatures.

Under all operating conditions in this study, traction coefficients (*TC*) under fully flooded conditions exhibit a similar relationship for all greases and the base oil, which is as follows:

$$TC_{Li-C-PAO} > TC_{PU-PAO} > TC_{Li-S-PAO} > TC_{PAO}.$$

The stable traction coefficients under starved conditions are shown in Fig. 9. Compared to fully flooded condition, the traction coefficients under starved condition are more sensitive to operating conditions for all tested greases. Specifically, within the operating conditions of this study, the maximum variation in traction coefficient under fully flooded condition is 0.006, 0.005, and 0.017 for Li-S-PAO, Li-C-PAO, and PU-PAO, respectively. In contrast, the maximum variation under starved condition is 0.160, 0.025, and 0.018 for Li-S-PAO, Li-C-PAO, and PU-PAO, respectively.

Notably, although Li-S-PAO maintains the lowest traction coefficient under fully flooded conditions in this study, the traction coefficient under starved conditions is particularly sensitive to operating conditions. Compared to fully flooded condition, the traction coefficient under starved condition shows not only a dramatic increase at u_r= 200 mm/s and T= 40°C, but also an even lower value at u_r= 200 mm/s and T= 80°C.

Due to the divergent traction coefficients of Li-S-PAO, the relationship among the tested greases becomes more complex under starved condition:

$\boldsymbol{TC_{Li-S-PAO}} \geq TC_{Li-C-PAO} > TC_{PU-PAO} > TC_{PAO}$ at u_r= 200 mm/s and T= 40°C; and u_r= 600 mm/s and T= 40°C;

$TC_{Li-C-PAO} > TC_{PU-PAO} > \boldsymbol{TC_{Li-S-PAO}} \approx TC_{PAO}$ at u_r= 200 mm/s and T= 80°C;

$TC_{Li-C-PAO} > \boldsymbol{TC_{Li-S-PAO}} > TC_{PU-PAO} > TC_{PAO}$ at u_r= 600 mm/s and T= 80°C.

It can be observed that the relationship between greases and base oil is highly dependent on the operating condition.

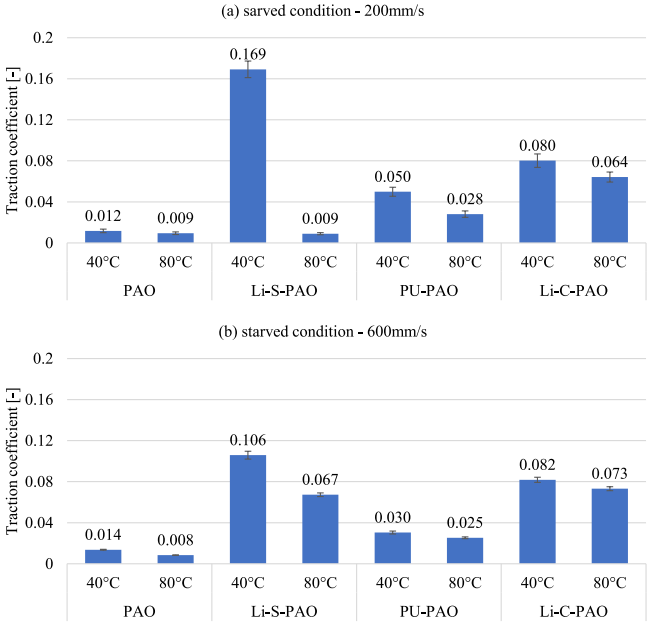

Fig. 9. Stable traction coefficient under starved conditions (traction coefficients of base oil are tested under fully flooded conditions), (a) u_r= 200 mm/s, (b) u_r= 600 mm/s.

In summary, the grease supply condition has a considerable effect on the stable traction coefficients. Specifically, under fully flooded condition, the traction coefficients have a consistent relationship for the tested greases, with Li-S-PAO maintaining the lowest traction coefficient under all operating conditions in this study. In contrast, under starved condition, this relationship no longer holds, and the grease with the lowest traction coefficient strongly depends on the operating conditions. These findings are consistent with bearing-level friction measurements reported by Muennich and Gloeckner in [47]. They show that under fully flooded condition, the friction torques induced by various greases follow a consistent relationship and remain higher than that of the base oil when the rolling speed exceeds approximately 150 mm/s. In contrast, under starved conditions, this relationship becomes more complex, particularly at higher speeds.

This indicates that when using a ball-on-disk tribometer to prescreen greases for rolling bearings, it is not sufficient to rely solely on friction measurements under fully flooded condition, because grease-lubricated rolling bearing generally operate under starved condition, and the grease supply condition has a considerable effect on the friction behavior. The potential mechanisms underlying these differences are discussed in the following section.

3.2. Dependence of friction behavior on grease film under starvation

In the last section, the effect of supply conditions on the traction coefficient during overrolling and their stable values are presented for various operating conditions and greases. In this section, the underlying mechanisms are discussed by correlating the measured traction coefficient with the formed grease film.

As shown in Fig. 4 to Fig. 7, at the beginning of overrolling, grease supply condition dose not significantly affect traction behavior. As indicated by Cann [16,27,29,48], at the beginning of overrolling, bulk grease is entrained into contact under both grease supply conditions. Additionally, according to measurements of film thickness reported in [49], similar film thicknesses can be formed under both fully flooded and starved conditions at the beginning of overrolling. In summary, formed grease films under both supply conditions exhibit similar components and thicknesses at the beginning of overrolling. Therefore, similar traction coefficients can be observed.

As overrolling continues, a nearly constant traction coefficient during overrolling is observed under fully flooded condition. Under this condition, the contact is continuously re-lubricated because of the scoop, and the contact area is consistently supplied with grease [14,25]. Therefore, the grease film remains unchanged [9,25]. Additionally, as shown in Fig. 8, the measured traction coefficient under fully flooded conditions is only slightly higher than that of base oil lubrication and decreases with increasing temperature. These observations are consistent with the conclusions reported in [5]. By correlating with film thickness, it is concluded the grease traction coefficient under fully flooded conditions is governed by the base oil viscosity within the so-called 'high-speed region' [5]. This 'high-speed region' encompasses the rolling speeds investigated in this study. Therefore, the correlation under fully flooded conditions is not repeatedly addressed in this study.

In contrast to fully flooded condition, where the dependence of traction behavior on grease film has been clarified in [5,8–11], such a study under starved condition is not yet available due to the lack of traction measurements. In the following two subsections, the measured traction coefficient and film thickness are correlated to clarify the dependence of traction behavior on grease film under starved condition.

3.2.1. Dependence during overrolling

Similar to the friction behavior during overrolling, Li-C-PAO is used as a representative example to avoid extensive repetition, because all three greases tested in this study show similar behaviors. The grease film thicknesses of two other greases are provided in the Appendix 5.2.

The traction coefficient and grease film thickness during overrolling are shown simultaneously in Fig. 10. As indicated in [23–25], grease lubrication during overrolling can be divided into two phases: the churning phase and the bleeding phase. The churning phase is characterized by a rapid decrease in film thickness [14]. As shown in Fig. 10, the churning phase continues until approximately 1700 disk revolutions. During the churning phase, some fresh grease is entrained into the contact area, while most of the grease is displaced to the sides of the track [26]. The entrained grease at the track center is continuously squeezed by the contact pressure. Driven by the contact-pressure gradient, the base oil flows laterally to the sides through the porous structure of thickener, as simulated in [15,24]. Consequently, the thickener concentration in the residual grease at the track center increases during overrolling [20,24]. Eventually, a solid-like thickener-rich layer is formed [6,16,17,20,22,30,38,42,44,48]. The increase of thickener concentration also leads to a significant rise of viscosity [15,17,24]. Therefore, the dramatic increase of traction coefficient at first 700 disk revolutions can be attributed to the formation of thickener-rich layer during the churning phase.

As overrolling continues, the grease film thickness remains nearly constant. A nearly constant film thickness indicates no considerable oil film is formed during the bleeding phase, although fluctuations in film thickness are observed. These fluctuations can be attributed to the presence of thickener particles in the contact zone. Except for these fluctuation events, the thickener-rich layer continues to dominate the separation of the contact surface until the end of the test. Therefore, the traction coefficient remains stable under this operating condition.

Notably, the turning point from churning phase to bleeding phase of the traction coefficient occurs earlier than that of film thickness. This can be attributed to that the disk materials in MTM and EHD2 tribometer are different. Therefore, the contact pressure in measuring traction coefficient is higher than that in measuring film thickness. A higher contact pressure promotes the formation of a thickener-rich layer, as demonstrated by experimental measurements in [44]. Consequently, the turning point of the traction coefficient occurs earlier than that of film thickness.

At a higher operating temperature of 80°C, the traction coefficient and grease film thickness are shown in Fig. 11. Under this condition, the churning phase in film thickness measurement ends at approximately 800 disk revolutions. Consequently, the traction coefficient increases during the first approximately 300 disk revolutions due to the previously mentioned increase in thickener concentration and viscosity of the thickener-rich layer. In comparison to 40°C, the churning phase ends earlier, because a higher temperature reduces the resistance of oil flowing through the porous structure of thickener [50]. As a result, the thickener-rich layer can be formed with less disk revolutions.

During the bleeding phase, in contrast to the stable grease film thickness at 40°C, the grease film thickness at 80°C increases gradually during overrolling. Additionally, film thickness fluctuations induced by the thickener particles is absent at 80°C. Both observations can be attributed to the formation of a higher thickness of oil film. When the viscosity becomes lower at higher temperature, more bled oil is available to form an oil film component [29,50]. In addition, the reduction in viscosity can decrease film thickness. Under severe starved condition and in the mixed lubrication regime, if the effect of bleeding promotion cannot compensate for the effect of viscosity reduction, the friction may increase as temperature increases. In this study, a thicker oil film is formed at 80°C. Therefore, the effect of bleeding promotion dominates. The viscosity of base oil is often 1000 times smaller than that of the thickener-rich layer [19,24]. When the oil film gradually separates the thickener-rich layers on both surfaces of disk and ball, the interaction between these two layers weakens. Consequently, consistent with the film thickness, the traction coefficient continuously decreases during the bleeding phase. In compared to 40°C where the traction is mainly induced by the thickener-rich layer, the traction coefficient at 80°C is reduced considerably after 1000 disk revolution due to the formation of oil film.

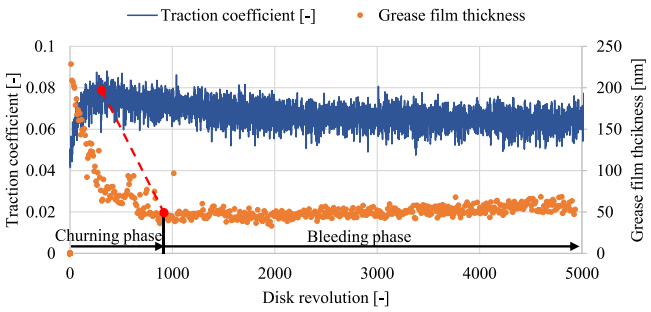

Fig. 11. Dependence of traction coefficient on grease film thickness during overrolling under starvation, with turning points marked with red dots (Li-C-PAO; u_r=200 mm/s; T=80°C).

To confirm the correlation between traction behavior and grease film thickness, the traction coefficient and grease film thickness measured at a higher rolling speed (u_r=600 mm/s) and under two operating temperatures are shown in Fig. 12 and Fig. 13, respectively.

Similar to the correlation observed at 200 mm/s and 40°C, during the churning phase at 600 mm/s and 40°C in Fig. 12, the film thickness decreases while the traction coefficient increases. Subsequently, a relatively stable grease film is formed. Correspondingly, the traction coefficient stabilizes until the end of the test. At 600 mm/s and 80°C in Fig. 13, the correlation between the traction coefficient and film thickness is also similar to that observed under a rolling speed of 200 mm/s at 80°C. The film thickness decreases during the churning phase, then recovers during the subsequent bleeding phase. In accordance with changes in film thickness, the traction coefficient initially increases before subsequently decreasing.

Additionally, in comparison to other operating conditions, the churning phase at 600 mm/s and 40°C requires more disk revolutions,

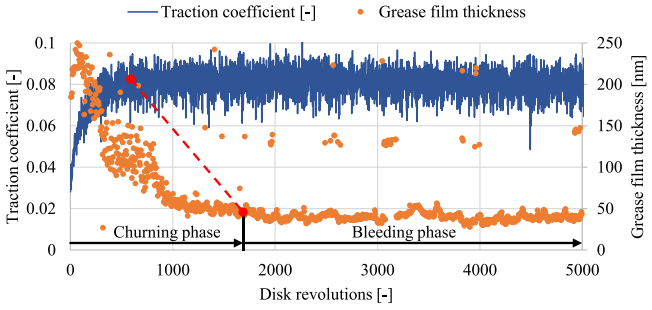

Fig. 10. Dependence of traction coefficient on grease film thickness during overrolling under starvation, with turning points marked with red dots (Li-C-PAO; u_r=200 mm/s; T = 40°C).

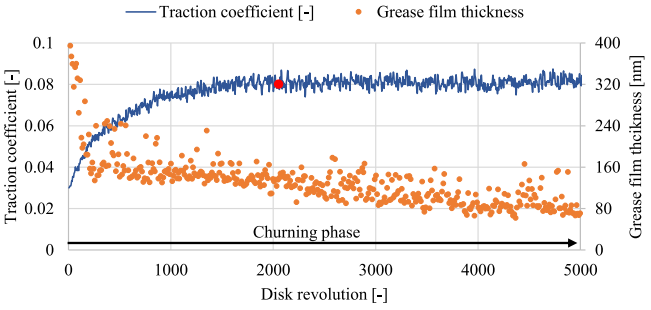

Fig. 12. Dependence of traction coefficient on grease film thickness during overrolling under starvation, with turning points marked with red dots (Li-C-PAO; u_r=600 mm/s; T=40°C).

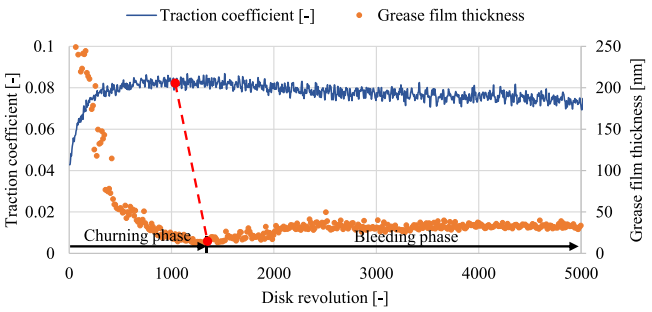

Fig. 13. Dependence of traction coefficient on grease film thickness during overrolling under starvation, with turning points marked with red dots (Li-C-PAO; u_r=600 mm/s; T=80°C).

as shown in Fig. 12. The film thickness does not stabilize even after 5000 disk revolutions. One possible reason is the higher overrolling frequency associated with increased rolling speeds [42]. When the rolling frequency is higher, the time for oil flowing through the porous structure of thickener becomes shorter during each overrolling. Another reason can be attributed to the lower temperature, which increases the viscosity of the base oil and thereby increases the resistance to oil flow within the thickener structure [51]. Consequently, additional disk revolutions are required to form a thickener-rich layer during the churning phase at 600 mm/s and 40°C, and the resulting film thickness is higher than that at 600 mm/s and 80°C.

In summary, under starved condition, the traction coefficient during overrolling depends on the evolution of grease film. During the churning phase, the dramatic increase in the traction coefficient can be attributed to the formation of a thickener-rich layer, which possesses a very high concentration of thickener and viscosity. During the bleeding phase, the traction coefficient can decrease when the oil film is formed efficiently. Additionally, the maximum values of the traction coefficient occur at the turning point from the churning phase to the bleeding phase, where the grease film primarily consists of a thickener-rich layer. Once formed, this layer is speed- and temperature-independent [43,44,51]. Therefore, the maximum traction coefficients under all tested operating conditions are nearly identical.

3.2.2. *Dependence under stable state*

As aforementioned, the stable traction coefficients under starved conditions are more sensitive to operating conditions. In this subsection, the underlying mechanisms are discussed by correlating the stable traction coefficient with the stable grease film. The film thicknesses at two operating temperatures are shown in Fig. 14. As discussed in the previous subsection, there are two components of the grease film: the thickener-rich layer and the oil film. For better illustration, the thicknesses of both components are plotted separately for all tested greases. Additionally, the Hamrock-Dowson equations are employed to calculate the lubricating film thickness formed by the base oil [52]. The accuracy of these equations has been validated for the conditions considered in this study [45].

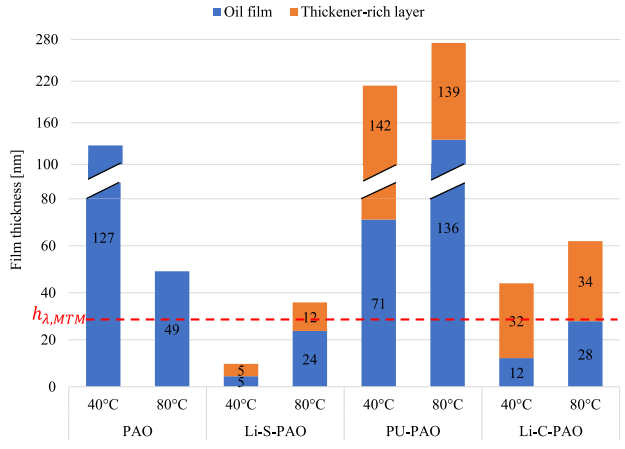

Fig. 14. Stable grease film under starved conditions when u_r= 200 mm/s.

First of all, it can be observed that the total grease film thickness formed by Li-S-PAO at 200 mm/s and 40°C is lower than the critical film thickness of traction measurement ($h_{\lambda,MTM}$), which indicates the occurrence of asperity contact. In contrast, grease films formed by all other greases exceed the $h_{\lambda,MTM}$. This explains why the traction coefficient induced by Li-S-PAO under this condition is significantly higher than those of all other greases and conditions, as shown in Fig. 9(a).

Additionally, as shown in Fig. 14, the thicknesses of oil films formed by greases are lower than those formed by base oil PAO, except for PU-PAO grease which will be discussed later. This indicates that the amount of bled oil remains insufficient. Therefore, when the operating temperature increases from 40°C to 80°C, the lower viscosity promotes additional bleeding of oil, allowing for a thicker oil film to be formed. Furthermore, when the operating temperature increases, the total grease film thickness, which is a superposition of thickener-rich layer and oil film, increases considerably for all tested greases, as shown in Fig. 14. This increase can primarily be attributed to an increase in oil film because changes in thickener-rich layer remain slight across both operating temperatures. Therefore, increasing the operating temperature not only reduces the viscosity of oil film, but more importantly, promotes the formation of oil film to reduce the traction between thickener-rich layers. Consequently, the traction coefficient decreases at a higher operating temperature, as shown in Fig. 9(a).

Therefore, the high sensitivity of the traction coefficient under starved conditions can be attributed to its dependence not only on the thickness of the grease film, but also on the both components of the grease film. When the grease film thickness is insufficient to avoid asperity contact, the traction coefficient is maximized. Within the full film lubrication regime, when the thickener-rich layer dominates the grease film, such as in the case of Li-C-PAO at 200 mm/s and 40°C, the traction coefficient is considerably higher than that of base oil lubrication, as shown in Fig. 9(a). In contrast, in the case of Li-S-PAO at 200 mm/s and 80°C, the thickness of the oil film is nearly twice that of the thickener-rich layer. The formed oil film can effectively reduce traction induced by the thickener-rich layers on both disk and ball surfaces. Therefore, under this condition, the traction coefficient is reduced to a value comparable to that of base oil lubrication, as shown in Fig. 9 (a).

In summary, for each grease working under starved condition, the correlation between the traction coefficients (TC) induced by asperity contact and both components is as follows:

$$TC_{asperity\ contact} > TC_{thickener-rich\ layer} > TC_{oil\ film}.$$

To verify the aforementioned correlation, the stable grease film thickness at a higher rolling speed is shown in Fig. 15. For Li-S-PAO, the total grease film at 600 mm/s and 40°C is higher than that at 200 mm/s and 40°C, but remains thinner than the critical film thickness ($h_{\lambda,MTM}$). Therefore, under this condition, the traction force is reduced but continues to be partially attributed to asperity contact. Consequently, it remains considerably higher than that of all other greases, as shown in Fig. 9(b). At a rolling speed of 600 mm/s and a temperature of 80°C, the thicknesses of both components increase while asperity contact is eliminated. Therefore, the traction coefficient is reduced significantly compared to that at 600 mm/s and 40°C. Additionally, the thicknesses of oil films formed by Li-S-PAO are lower than those formed by base oil PAO. This indicates that the amount of bled oil remains insufficient. When the bled oil volume is insufficient, the oil film thickness decreases with increasing rolling speeds [53–55]. Consequently, the traction coefficient increases as rolling speeds rise.

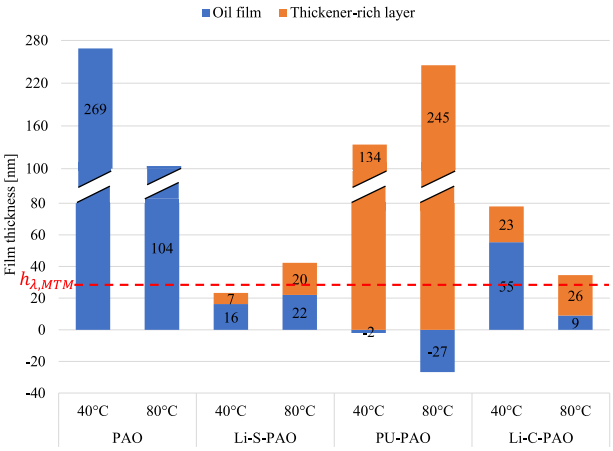

Fig. 15. Stable grease film under starved conditions when u_r= 600 mm/s.

For Li-C-PAO, the thickness of oil film at 600 mm/s and 40°C is higher than that at 200 mm/s and 40°C, as shown in Fig. 15. According to aforementioned relationship, the traction coefficient at 600 mm/s and 40°C should be lower. However, it is actually comparable to that at 200 mm/s and 40°C, as shown in Fig. 9. This derivation can be attributed to the measurement method of thickener-rich layer. As shown in Fig. 12, the film thickness remains unstable even after 5000 disk revolutions. Therefore, it is reasonable to believe the churning phase has not finished by the end of the test, and thickener-rich layer still has a high oil saturation. Consequently, when measuring the thickness of the thickener-rich layer under standstill conditions, some base oil is squeezed out from this layer, resulting in a lower thickness than its actual value during overrolling. In other words, a higher thickness of oil film is measured than the actual value during overrolling. At 600 mm/s and 80°C in Fig. 15, the thickness of oil film is lower compared to that at 200 mm/s and 80°C, because of insufficient bled oil volume. Consequently, the traction coefficient becomes higher when rolling speed increases, as shown in Fig. 9. This observation aligns with the previously mentioned correlation.

The aforementioned correlation also explains the difference of between Li-S-PAO and Li-C-PAO. As shown in Figs. 14 and 15, the grease film formed by Li-C-PAO is sufficient to avoid the mixed lubrication at 40°C, while the contact lubricated using Li-S-PAO operates in mixed lubrication regime. Therefore, Li-C-PAO reduces the traction coefficient at 40°C. When the temperature increases to 80°C, the thickness of the thickener-rich layer formed by Li-C-PAO is much higher than that formed by Li-S-PAO at 200 mm/s, but only slightly higher at 600 mm/s. This pattern can be attributed to the difference in the thickener concentration. As indicated in [24], a higher thickener concentration can promote the formation of thickener-rich layer. Therefore, at 80°C the traction coefficient of Li-C-PAO is much higher than that of Li-S-PAO at 200 mm/s (see Fig. 14) and slightly higher at 600 mm/s (see Fig. 15). Additionally, it should be noticed that the correlation between traction behavior and grease film in this study is concluded for a given grease working under various conditions. The effect of thickener concentration on this correlation should be further studied.

For PU-PAO, an increase in temperature also results in a thicker grease film, as shown in Fig. 15, which indicates an increase in the oil film. Correspondingly, the traction coefficient decreases at elevated temperatures, as shown in Fig. 9. This observation is consistent with those of the other two greases. Additionally, the measured thicknesses of the thickener-rich layer are significantly greater than those of the other two greases. The possible reason can be attributed to the fact that polyurea thickener exhibits excellent adhesive properties on chromium surfaces [38]. Furthermore, the thickener-rich layer formed by PU-PAO is relatively soft [38]. Consequently, the measured thicknesses of the thickener-rich layer formed by PU-PAO exhibit significant variation despite additional measurements being taken. This may explain why the measured thickness of oil film exceeds that of base oil at 200 mm/s and 80°C in Fig. 14. It may also account for negative values observed for oil film thickness at a rolling speed of 600 mm/s in Fig. 15.

In summary, to minimize the traction coefficient under starved conditions, the PU-PAO and Li-C-PAO greases are recommended at the lower temperature in this study, because they can form sufficient grease film thickness to prevent asperity contact. In contrast, at the higher temperature, the Li-S-PAO grease can be considered, because its oil film component is dominated in the formed grease film. Meanwhile, it should be noted that traction coefficient of Li-S-PAO grease under starved condition is sensitive to operating conditions. Therefore, when pre-screening greases, it is essential to conduct the tribometer tests under starved condition, which is a more practical condition in grease-lubricated rolling bearings.

4. Conclusions

The ball-on-disk tribometer test is considered as a modern method for evaluating the lubricity of grease-lubricated rolling bearings. However, current tribometer tests are typically conducted under fully flooded conditions, whereas the grease supplied to contacts in rolling bearings is often starved. This study aims to clarify whether grease supply conditions affect friction behavior and to study the correlation between friction and grease film under starved condition. To achieve this aim, two ball-on-disk tribometers, MTM and EHD2, are used to measure traction coefficient and film thickness, respectively. The key findings can be summarized as follows:

1) The supply condition significantly affects the friction behavior of grease-lubricated rolling contact. The traction coefficient under fully flooded conditions exhibits only slight variations during overrolling, whereas significant changes are observed under starved conditions. Under fully flooded conditions, the stable traction coefficients have a consistent relationship. However, under starved conditions, this relationship is not valid, and traction coefficients are more sensitive to the operating conditions.
2) Under staved conditions, the traction coefficient during overrolling depends on the evolution of grease film. During the churning phase, the formation of a thickener-rich layer leads to a higher traction coefficient. Subsequently, during the bleeding phase, the formation of an oil film can reduce the traction coefficient.
3) Under starved conditions, the stable traction coefficient depends not only on the thickness of the grease film but also on both components of the grease film. Under the full film lubrication regime, an increase in the thickness of the oil film component can reduce the traction coefficient.

The findings from this study highlight the essential role of tribometer tests conducted under starved lubrication for pre-screening greases, because grease-lubricated rolling bearings typically operate under this condition. However, it remains unclear whether the starved condition reproduced on the ball-on-disk tribometer faithfully reflects that in practical grease-lubricated rolling bearings. As an outlook, the results obtained in this study will be compared with those from a bearing test rig to assess the transferability of the tribometer tests.

5. Statement of originality

On behalf of my co-authors, I declare that the work described in the manuscript “Friction behavior of grease-lubricated rolling contact and its dependence on grease film under starvation” has not been published previously in any other journal and neither is under consideration for publication in any other journal.

CRediT authorship contribution statement

Shuo Zhang: Writing – review & editing, Writing – original draft, Visualization, Software, Methodology, Investigation, Data curation, Conceptualization. **Benjamin Klinghart:** Writing – review & editing, Visualization, Methodology, Investigation. **Georg Jacobs:** Writing – review & editing, Supervision, Project administration, Investigation, Funding acquisition, Conceptualization. **Jianlong Xiao:** Writing – original draft, Methodology, Investigation. **Yujun Wang:** Writing – review & editing, Writing – original draft, Investigation. **Florian König:** Writing – review & editing, Supervision, Methodology, Investigation, Funding acquisition, Conceptualization. **Marius Bürger:** Writing – review & editing, Methodology.

Declaration of Competing Interest

The authors declare that they have no known competing financial interests or personal relationships that could have appeared to influence the work reported in this paper.

Acknowledgements

The authors would like to thank the German Federal Ministry for Economic Affairs and Climate Action (IGF Vorhaben Nr.: 21063 N) as well as the Research Association for Drive Technology FVA (Forschungsvereinigung Antriebstechnik e. V., Nr.: 580 IV) for supporting this study.

Federal Ministry for Economic Affairs and Climate Action

FVA Forschungsvereinigung Antriebstechnik e.V.

Novelty Statement

On behalf of my co-authors, I declare that the work described in the manuscript

"Friction behavior of grease-lubricated rolling contact and its dependence on grease film under starvation" has not been published previously in any other journal and neither is under consideration for publication in any other journal.

Appendix

Friction behavior during overrolling

When grease Li-S-PAO is used as the lubricant, the traction coefficients during overrolling under two supply conditions are shown in Figs. 16–19. Similar to grease Li-C-PAO, the traction coefficients exhibit only slight variations during overrolling under fully flooded conditions, whereas significant changes are observed under starved conditions. Specifically, under starved conditions, the traction coefficient increases at the beginning of overrolling subsequently remines approximately constant at 40°C or decreases at 80°C.

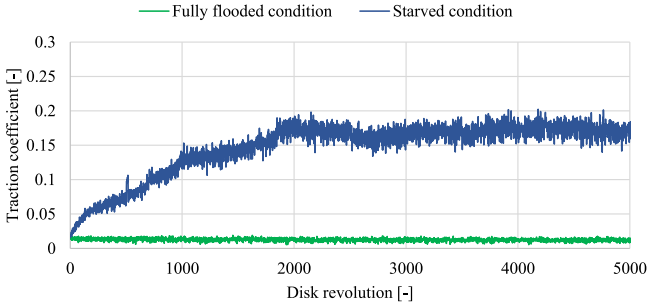

Fig. 16. Traction coefficients during overrolling under two supply conditions (Li-S-PAO; u_r=200 mm/s; T = 40°C)

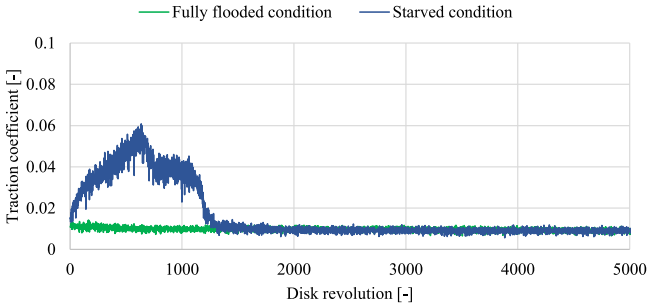

Fig. 17. Traction coefficients during overrolling under two supply conditions (Li-S-PAO; u_r=200 mm/s; T = 80°C)

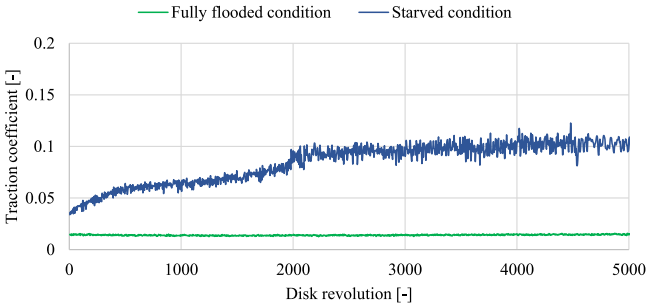

Fig. 18. Traction coefficients during overrolling under two supply conditions (Li-S-PAO; u_r=600 mm/s; T = 40°C)

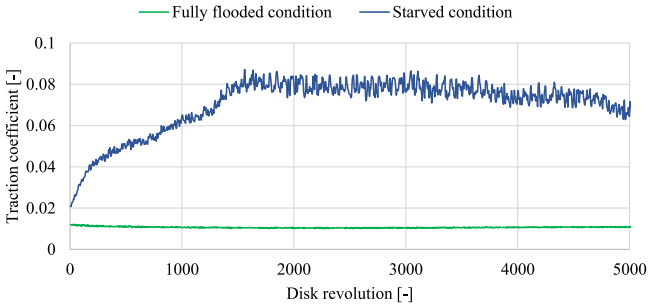

Fig. 19. Traction coefficients during overrolling under two supply conditions (Li-S-PAO; u_r=600 mm/s; T = 80°C)

When grease PU-PAO is used as the lubricant, the traction coefficients during overrolling under two supply conditions are shown in Figs. 20–23. Similar to grease Li-C-PAO, the traction coefficients exhibit only slight variations during overrolling under fully flooded conditions, whereas significant changes are observed under starved conditions. Specifically, under starved conditions, the traction coefficient increases at the beginning of overrolling subsequently remines approximately constant at 40°C or decreases at 80°C. Although the decrease of the traction coefficient at 600 mm/s and 80°C is not obvious, the coefficient remains considerably lower than that at 600 mm/s and 40°C.

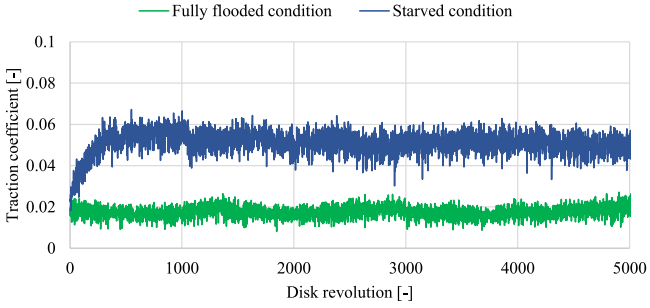

Fig. 20. Traction coefficients during overrolling under two supply conditions (PU-PAO; u_r=200 mm/s; T = 40°C)

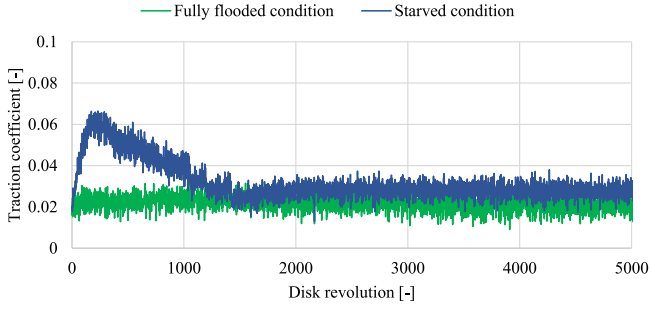

Fig. 21. Traction coefficients during overrolling under two supply conditions (PU-PAO; u_r=200 mm/s; T = 80°C)

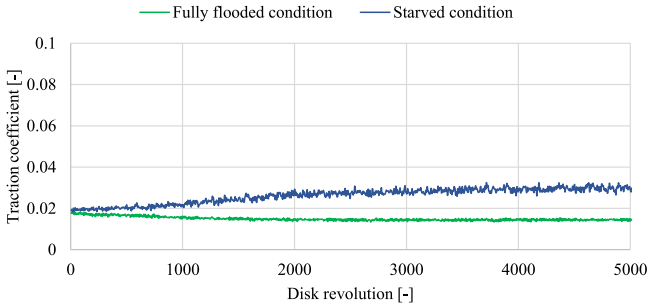

Fig. 22. Traction coefficients during overrolling under two supply conditions (PU-PAO; u_r=600 mm/s; T = 40°C)

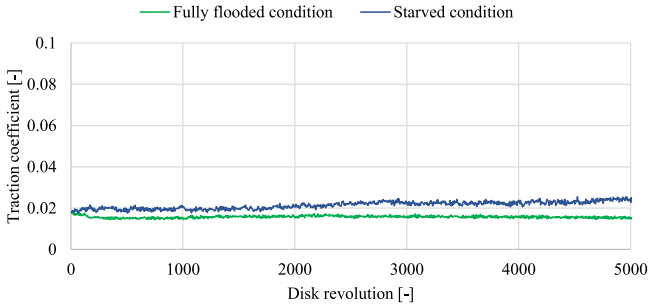

Fig. 23. Traction coefficients during overrolling under two supply conditions (PU-PAO; u_r=600 mm/s; T = 80°C)

Dependence of friction behavior on grease film under starvation during overrolling

When grease Li-S-PAO is used as the lubricant, the dependence of friction behavior on the grease film under starvation is shown in Figs. 24–27. Similar to grease Li-C-PAO, during the churning phase, the formation of a thickener-rich layer leads to a higher traction coefficient. Subsequently, during the bleeding phase, traction coefficient is reduced when an oil film can be formed with sufficient film thickness at a higher temperature.

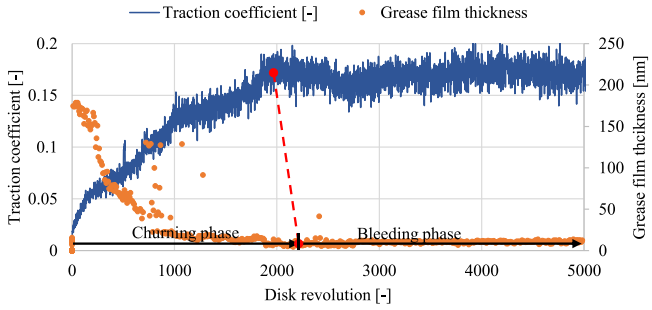

Fig. 24. Dependence of traction coefficient on grease film thickness during overrolling under starvation, with turning points marked with red dots (Li-S-PAO; u_r=200 mm/s; T = 40°C)

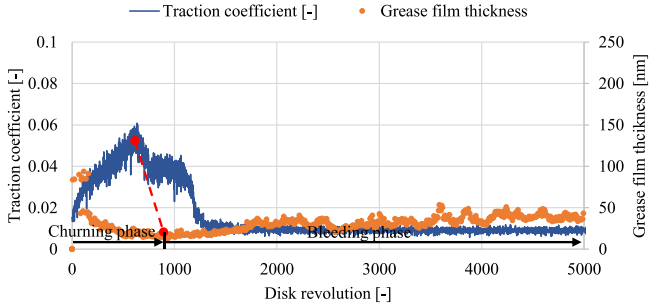

Fig. 25. Dependence of traction coefficient on grease film thickness during overrolling under starvation, with turning points marked with red dots (Li-S-PAO; u_r=200 mm/s; T = 80°C)

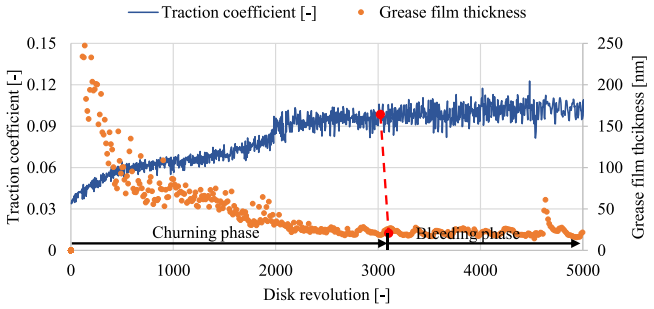

Fig. 26. Dependence of traction coefficient on grease film thickness during overrolling under starvation, with turning points marked with red dots (Li-S-PAO; u_r=600 mm/s; T = 40°C)

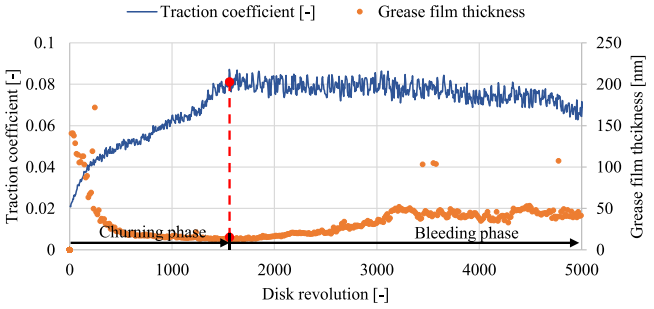

Fig. 27. Dependence of traction coefficient on grease film thickness during overrolling under starvation, with turning points marked with red dots (Li-S-PAO; u_r=600 mm/s; T = 80°C)

When grease PU-PAO is used as the lubricant, the dependence of friction behavior on the grease film under starvation is shown in Figs. 28–31. Similar to grease Li-C-PAO, during the churning phase, the formation of a thickener-rich layer leads to a higher traction coefficient. Subsequently, during the bleeding phase, the traction coefficient is reduced when an oil film can be formed with sufficient film thickness at a higher temperature. Fluctuation in grease film thickness can be attributed to the presence of thickener particles, as explained in Section 3.2.

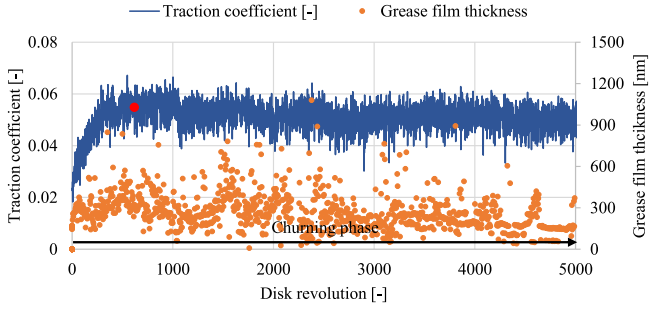

Fig. 28. Dependence of traction coefficient on grease film thickness during overrolling under starvation, with turning points marked with red dots (PU-PAO; u_r=200 mm/s; T = 40°C)

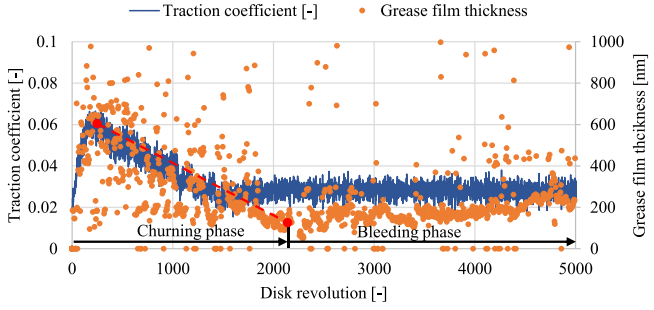

Fig. 29. Dependence of traction coefficient on grease film thickness during overrolling under starvation, with turning points marked with red dots (PU-PAO; u_r=200 mm/s; T = 80°C)

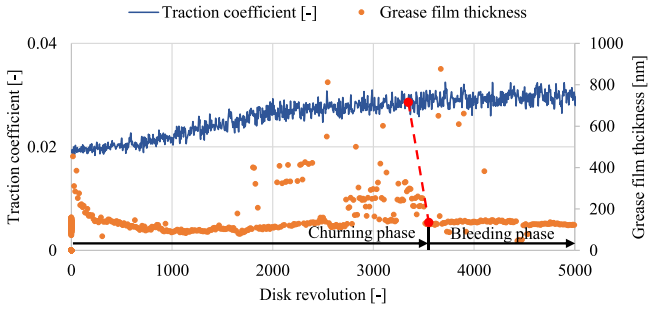

Fig. 30. Dependence of traction coefficient on grease film thickness during overrolling under starvation, with turning points marked with red dots (PU-PAO; u_r=600 mm/s; T = 40°C)

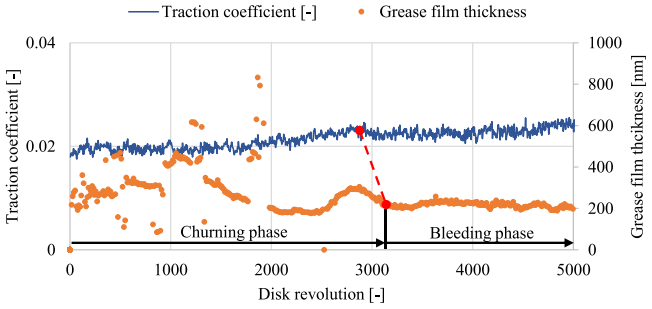

Fig. 31. Dependence of traction coefficient on grease film thickness during overrolling under starvation, with turning points marked with red dots. (PU-PAO; u_r=600 mm/s; T = 80°C)

References

[1] Holmberg K, Erdemir A. Influence of tribology on global energy consumption, costs and emissions. Friction 2017;5(3):263–84. https://doi.org/10.1007/s40544-017-0183-5.

[2] International Organization for Standardization. Rolling bearings - Dynamic load ratings and rating life(ISO 281:2007). Berlin: Beuth Verlag GmbH. https://doi.org/10.31030/1718715.

[3] Lugt PM. A review on grease lubrication in rolling bearings. Tribology Trans 2009;52(4):470–80. https://doi.org/10.1080/10402000802687940.

[4] Lugt PM. Modern advancements in lubricating grease technology. Tribology Int 2016;97:467–77. https://doi.org/10.1016/j.triboint.2016.01.045.

[5] Laurentis N de, Kadiric A, Lugt P, Cann P. The influence of bearing grease composition on friction in rolling/sliding concentrated contacts. Tribology Int 2016;94:624–32. https://doi.org/10.1016/j.triboint.2015.10.012.

[6] Cann PM. Grease lubrication of rolling element bearings - Role of the grease thickener. Lubr Sci 2007;19(3):183–96. https://doi.org/10.1002/ls.39.

[7] Vengudusamy B, Enekes C, Spallek R. On the film forming and friction behaviour of greases in rolling/sliding contacts. Tribology Int 2019;129:323–37. https://doi.org/10.1016/j.triboint.2018.08.026.

[8] Gonçalves D, Graça B, Campos AV, Seabra J. On the friction behaviour of polymer greases. Tribology Int 2016;93:399–410. https://doi.org/10.1016/j.triboint.2015.09.027.

[9] Gonçalves D, Vieira A, Carneiro A, Campos A, Seabra J. Film thickness and friction relationship in grease lubricated rough contacts. Lubricants 2017;5(3):34. https://doi.org/10.3390/lubricants5030034.

[10] Laurentis N de, Cann P, Lugt PM, Kadiric A. The influence of base oil properties on the friction behaviour of lithium greases in rolling/sliding concentrated contacts. Tribology Lett 2017;65(4). https://doi.org/10.1007/s11249-017-0908-7.

[11] Kanazawa Y, Laurentis N de, Kadiric A. Studies of friction in grease-lubricated rolling bearings using ball-on-disc and full bearing tests. Tribology Trans 2020;63(1):77–89. https://doi.org/10.1080/10402004.2019.1662147.

[12] Cann PM. Grease degradation in a bearing simulation device. Tribology Int 2006;39(12):1698–706. https://doi.org/10.1016/j.triboint.2006.01.029.

[13] Baly H, Poll G, Cann PM, Lubrecht AA. Correlation between model test devices and full bearing tests under grease lubricated conditions. IUTAM Symp Elastohydrodyn MicroElastohydrodyn Solid Mech Appl 2006:134.

[14] Fischer D, Jacobs G, Stratmann A, Burghardt G. Effect of base oil type in grease composition on the lubricating film formation in EHD contacts. Lubricants 2018;6(2):32. https://doi.org/10.3390/lubricants6020032.

[15] Nogi T, Soma M, Dong D. Numerical analysis of grease film thickness and thickener concentration in Elastohydrodynamic lubrication of point contacts. Tribology Trans 2020;63(5):924–34. https://doi.org/10.1080/10402004.2020.1778147.

[16] Cann PM. Starvation and reflow in a grease-lubricated elastohydrodynamic contact. Tribology Trans 1996;39(3):698–704. https://doi.org/10.1080/10402009608983585.

[17] Kochi T, Sakai M, Nogi T, Dong D, Kimura Y. Experimental study on the physics of thick EHL film formation with grease at low speeds. Tribology Lett 2019;67(2):589. https://doi.org/10.1007/s11249-019-1166-7.

[18] Okal M, Kostal D, Osara JA, Lugt PM, Krupka I, Hartl M. Experimental study of the effect of thickener on the film thickness in the contacts of a grease-lubricated rolling ball bearing at low speed. Tribology Trans 2024:1–13. https://doi.org/10.1080/10402004.2024.2431523.

[19] Tichy J, Menut M, Oumahi C, Muller S, Bou-Saïd B. Grease flow based on a two-component mixture model. Tribology Int 2021;153(A):106638. https://doi.org/10.1016/j.triboint.2020.106638.

[20] Okal M, Kostal D, Sakai K, Krupka I, Hartl M. Thickener behaviour in rolling Elastohydrodynamic lubrication contacts. Tribology Lett 2024;72(3):72. https://doi.org/10.1007/s11249-024-01874-0.

[21] Yeong SK, Luckham PF, Tadros TF. Steady flow and viscoelastic properties of lubricating grease containing various thickener concentrations. J Colloid Interface Sci 2004;274(1):285–93. https://doi.org/10.1016/j.jcis.2004.02.054.

[22] Vengudusamy B, Kuhn M, Rankl M, Spallek R. Film forming behavior of greases under starved and fully flooded EHL conditions. Tribology Trans 2016;59(1):62–71. https://doi.org/10.1080/10402004.2015.1071450.

[23] Mérieux J-S, Hurley S, Lubrecht AA, Cann PM. Shear-degradation of grease and base oil availability in starved EHL lubrication. Tribology Ser 2000;38:581–8. https://doi.org/10.1016/S0167-8922(00)80162-5.

[24] Zhang S, Klinghart B, Jacobs G, Goeldel S von, König F. Prediction of bleeding behavior and film thickness evolution in grease lubricated rolling contacts. Tribology Int 2024;193:109369. https://doi.org/10.1016/j.triboint.2024.109369.

[25] Li X, Guo F, Poll G, Fei Y, Yang P. Grease film evolution in rolling elastohydrodynamic lubrication contacts. Friction 2021;9(1):179–90. https://doi.org/10.1007/s40544-020-0381-4.

[26] Aström H, Östensen JO, Höglund E. Lubricating grease replenishment in an Elastohydrodynamic point contact. J Tribology 1993;115(3):501–6. https://doi.org/10.1115/1.2921666.

[27] Cann PM. Starved Grease Lubrication of Rolling Contacts. Tribology Trans 1999;42(4):867–73. https://doi.org/10.1080/10402009908982294.

[28] Cann PM. Thin-film grease lubrication. Proc Inst Mech Eng Part J J Eng Tribology 1999;213(5):405–16. https://doi.org/10.1243/1350650991542776.

[29] Cann PM, Lubrecht AA. An analysis of the mechanisms of grease lubrication in rolling element bearings. Lubr Sci 1999;11(3):227–45. https://doi.org/10.1002/ls.3010110303.

[30] Hurley S, Cann PM. IR spectroscopic analysis of grease lubricant films in rolling contacts. Tribology Ser 1999;36:589–600. https://doi.org/10.1016/S0167-8922(99)80079-0.

[31] Huang L, Guo D, Wen S. Film thickness decay and replenishment in point contact lubricated with different greases: a study into oil bleeding and the evolution of lubricant reservoir. Tribology Int 2016;93:620–7. https://doi.org/10.1016/j.triboint.2014.11.005.

[32] Huang L, Guo D, Wen S. Starvation and reflow of point contact lubricated with greases of different chemical formulation. Tribology Lett 2014;55(3):483–92. https://doi.org/10.1007/s11249-014-0376-2.

[33] Lugt PM. Grease lubrication in rolling bearings. Hoboken, N.J.: John Wiley & Sons, Ltd; 2013.
[34] Baart P, van der Vorst B, Lugt PM, van Ostayen RA. Oil-bleeding model for lubricating grease based on viscous flow through a porous microstructure. Tribology Trans 2010;53(3):340–8. https://doi.org/10.1080/10402000903283326.
[35] Saatchi A, Shiller PJ, Eghtesadi SA, Liu T, Doll GL. A fundamental study of oil release mechanism in soap and non-soap thickened greases. Tribology Int 2017;110(2):333–40. https://doi.org/10.1016/j.triboint.2017.02.004.
[36] Zhang Q, Mugele F, Lugt PM, van den Ende D. Characterizing the fluid-matrix affinity in an organogel from the growth dynamics of oil stains on blotting paper. Soft Matter 2020;16(17):4200–9. https://doi.org/10.1039/c9sm01965k.
[37] Zhang Q, Mugele F, van den Ende D, Lugt PM. A model configuration for studying stationary grease bleed in rolling bearings. Tribology Trans 2021;64(6):1–11. https://doi.org/10.1080/10402004.2021.1904071.
[38] Huang L, Guo D, Liu X, Xie G, Wan GTY, Wen S. Effects of nano thickener deposited film on the behaviour of starvation and replenishment of lubricating greases. Friction 2016;4(4):313–23. https://doi.org/10.1007/s40544-016-0123-9.
[39] PCS Instruments. MTM2 Operation Manual.
[40] Shetty P, Meijer RJ, Lugt PM. An evaporation model for base oil from grease-lubricated rolling bearings including breathing. Tribology Trans 2021;64(5):891–902. https://doi.org/10.1080/10402004.2021.1943088.
[41] P.C.S. Instruments. EHD2 operation manual V2.0.
[42] Fischer D, Mues H, Jacobs G, Stratmann A. Effect of over rolling frequency on the film formation in grease lubricated EHD contacts under starved conditions. Lubricants 2019;7(2):19. https://doi.org/10.3390/lubricants7020019.
[43] Cann P.M., Lubrecht A., Venner C.H. Grease lubrication of rolling element bearings - A model future? International Tribology Conference 2000.
[44] Klinghart B, Jacobs G, König F. Einfluss des Verdickers auf die Schmierfilmhöhe in fettgeschmierten Wälzkontakten. VDI-Berichte; 2023. p. 235–46. https://doi.org/10.51202/9783181024157-235.
[45] Fischer D. Effects of base oil and thickener on the film formation in grease lubricated rolling contacts. Aachen; 2023.
[46] Allmaier H. Increase service life for rail wheel bearings - A review of grease lubrication for this application. Lubricants 2022;10(3):36. https://doi.org/10.3390/lubricants10030036.
[47] Muennich HC, Gloeckner HJR. Elastohydrodynamic lubrication of grease-lubricated rolling bearings. Tribology Trans 1980;23(1):45–52. https://doi.org/10.1080/05698198008982945.
[48] Cann PM. Understanding grease lubrication. Tribology Ser 1996;31:573–81. https://doi.org/10.1016/S0167-8922(08)70819-8.
[49] Gonçalves D, Campos A, Seabra J. An Experimental study on starved grease lubricated contacts. Lubricants 2018;6(3):82. https://doi.org/10.3390/lubricants6030082.
[50] Zhang S., Jacobs G., Klinghart B., König F. Film formation evolution in grease-lubricated rolling contacts: impact of operating temperatures. Conference Proceedings of 24th International Colloquium Tribology - Industrial and Automotive Lubrication 2024:131-132.
[51] Zhang S. Calculation of the lubricating film thickness in grease-lubricated rolling contacts. Aachen: RWTH Aachen University; 2024.
[52] Hamrock BJ, Dowson D. Isothermal Elastohydrodynamic lubrication of point contacts: Part III—Fully flooded results. J Lubr Technol 1977;99(2):264–75. https://doi.org/10.1115/1.3453074.
[53] Fischer D, Goeldel S von, Jacobs G, Stratmann A, König F. Investigation of lubricant supply in rolling point contacts under starved conditions using CFD simulations. IOP Conference Series Materials Science Engineering 2021;1097(1):12007. https://doi.org/10.1088/1757-899X/1097/1/012007.
[54] Nogi T. Film thickness and rolling resistance in starved Elastohydrodynamic lubrication of point contacts with reflow. J Tribology 2015;137(4):41502. https://doi.org/10.1115/1.4030203.
[55] Zhang S, Jacobs G, Goeldel S von, Vafaei S, König F. Prediction of film thickness in starved EHL point contacts using two-phase flow CFD model. Tribology Int 2023;178:108103. https://doi.org/10.1016/j.triboint.2022.108103.